

# Friction and Deformation of Nylon.

## I. Experimental

N. ADAMS,\* *British Rayon Research Association, Manchester, England*

### 1. INTRODUCTION

The observed dependence of friction on load for polymers is satisfactorily represented, over large load ranges, by an equation of the form  $F = \alpha W^n$  where  $F$  is the friction,  $W$  is the load, and  $\alpha$  and  $n$  are constants,  $n$  usually having a value between  $2/3$  and 1 (see e.g., Howell and Mazur<sup>1</sup>). Because, in the special case of  $n = 1$  this equation reduces to  $F = \mu W$ , it has been regarded as a more general form of Amontons' laws of friction and has been explained on the basis of the "adhesion theory" of friction which has successfully interpreted Amontons' laws.<sup>2</sup>

According to the adhesion theory the friction between rubbing bodies is closely related to their "true contact area," which may be defined as the area over which they are within range of one another's molecular forces. If the surfaces of the bodies are perfectly smooth, the true contact area is equal to the "apparent contact area" which is the area bounded by the line at which the two bodies diverge. The apparent contact area is determined by the macroscopic deformation of the bodies and is measurable. If, however, the surfaces are rough, contact can only occur at the tips of those asperities which lie within the apparent contact area. The true contact area is then determined by the deformation of these asperities and is consequently always smaller than the apparent contact area but approaches it as the surfaces tend toward perfect smoothness and as the average pressure on the contact increases.

Where the deformation of the asperities is "plastic," as is common for asperities on metal surfaces, Amontons' laws hold, but where the deformation of the asperities and the substrate is elastic a power-law relation between friction and load, similar to that observed for polymers, is predicted.<sup>3</sup>

Measurements made by Lincoln<sup>4</sup> and Pascoe and Tabor,<sup>5</sup> in which high average pressures were used so that an approximate equality between true and apparent contact area was expected, showed that the apparent contact area  $A$  was related to the load by an equation of the form  $A = \beta W^m$  where  $\beta$  and  $m$  are constants and  $m$  has a value similar to that of  $n$  measured for the same polymer. These results showed that for a broad description of polymer friction it is adequate to assume a constant shear strength, of value  $\beta/\alpha$ , for the true contact area.

\* Present address: A.E.R.E., Harwell, England.

The twin measurements of friction and apparent contact area in these measurements were made separately so that the friction did not act during the area measurement. This detracts from the firmness of their conclusions, because it is conceivable that the size of the contact area may be affected by the friction. For example, Parker and Hatch<sup>6</sup> showed that the presence of tangential forces can increase the contact areas between indium and lead hemispheres and a glass plate. On the other hand, it has been shown theoretically that a tangential force does not affect the size or shape of the contact areas of "Hookean" spheres.<sup>7</sup> Under the strains which polymers incur at friction contacts, their deformation is usually not Hookean, though it may be completely recoverable, and it is not clear what the effect of tangential force should be. Grosberg,<sup>8</sup> in a theory of the differential friction of wool, suggested that the apparent contact area of polymers is determined by the magnitude of the vectorial sum of the normal and tangential forces, but the experimental evidence on this point is not conclusive.<sup>5</sup>

In the present work a method is established for the measurement of apparent contact area between a polymer hemisphere and a rigid plane; it is free from some of the systematic errors of previous methods and can be employed during slow-speed sliding, permitting simultaneous measurement of contact area and friction.

## 2. EXPERIMENTAL DETAILS

Simultaneous measurements were made of the apparent contact area and kinetic friction between nylon hemispheres and a plane glass plate over a 200 to 1 load range. The effects of changes in sliding speed and in the duration of loading were also studied.

This contact geometry was selected, despite the nonuniformity of the normal pressure on the apparent contact area, in the expectation (based on the theoretical prediction for Hookean materials by Mindlin and Deresiewicz<sup>7</sup>) that the distribution of normal pressure over the apparent contact area would not be seriously affected by the presence of tangential forces. Also, the use of specimens of small radius of curvature enables high average pressure to be exerted on the apparent contact area with the use of conveniently low loads. High pressures conduce to the true contact area attaining equality with the apparent contact area.

The materials were selected for their mechanical and optical properties, the polished glass plate for its smoothness and high modulus ( $\sim 70$  times that of nylon) which together make the contributions to the measured friction from "ploughing" and "hysteresis" friction negligible, and the 610 polymer of nylon for the smooth surface that it is possible to give it. At least one of the materials had to be optically transparent (in fact, both were) to permit the measurement of the apparent contact areas by an interferometric method.

## 2.1. Specimen Preparation

The hemispherical nylon 610 specimens were prepared by melting nylon chips in indentations made by selected steel ball bearings of diameters  $\frac{3}{32}$  in.,  $\frac{3}{16}$  in., and  $\frac{7}{16}$  in. in small fine silver blocks which had been previously heavily gold-plated. Rapid quenching in iced water resulted in specimens which were optically clear and colorless. After soaking in water for 24 hr. the specimens separated cleanly from the molds and were found to possess a surface finish as good as the original ball bearings. It was found necessary to dry the nylon chips intensively, to prevent evolution of water vapor on melting, and to use an inert atmosphere ( $N_2$ ) during melting to prevent oxidation.

Both the specimen and the glass plate were extracted with petroleum ether (b.p. 60–80°C.) for 2 hr. and allowed to condition in air at 20°C. and 66% r.h. for 24 hr. before measurements were performed.

## 2.2. Apparatus

The essential feature of the apparatus with which the experiments were performed, Figure 1, lies in the method by which the friction between the nylon hemisphere and the glass plate is measured while their contact remains in the field of view of a microscope.

The glass plate is suspended from a rigid frame, by the kinematic spring systems A and B, so that its rubbing surface, which is vertical, is perpendicular to the microscope axis and lies in the field plane of the objective.

The nylon hemisphere is mounted from the base of the apparatus on a cross-spring hinge C which permits rotation only about a horizontal axis lying in the field plane and is a sufficient distance below the microscope

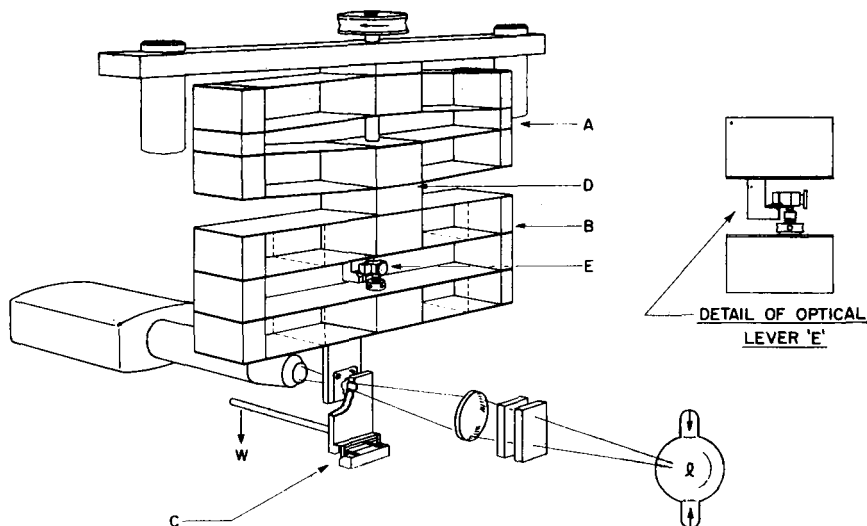


Fig. 1. General view of apparatus.

for the locus of the tip of the hemisphere to intersect the surface of the glass plate on the microscope axis.

Loads from 0 to 200° g.-wt. between the specimen and the glass plate are applied by placing weights on a horizontal arm projecting from the cross-spring hinge.

Relative motion between the specimen and the glass plate is produced by moving the plate. The spring systems A and B (which are similar to a design by Jones<sup>9</sup>) constrain the glass plate to move vertically—i.e., parallel to its surface—and offer great resistance to forces in perpendicular directions. This ensures that at all times the contact remains at the center of the microscope's field of view.

Movement of the glass plate is produced by a screw which engages a nut in the rigid frame and presses at its lower end, via a wobble pin, against the block D which connects the springs A and B. The screw was belt-driven from an electric motor through a gear box and could generate velocities of 9.5–330  $\mu$ /sec. Even when viewed at a linear magnification of 160 the glass plate moved smoothly.

Friction between the specimen and the glass plate extended or compressed the spring system B, according to the sense in which the glass plate was moving, and this deflection was measured by means of the sensitive lever E. The reflected beam from the optical lever and a reference beam reflected from a semialuminized mirror mounted in front of it were focused on the film plane of the microscope camera. Changes in the separation of the two foci were proportional to the changes of friction. To increase the range of friction that could be measured it was arranged that the stiffness of spring system B could be increased when required by halving the effective length of the cantilever springs of which it is composed. This was done by clamping metal blocks (dotted lines, Fig. 1) between the springs. Full-scale deflection was given by a force of 12 g.-wt. without the blocks and 80 g.-wt. when they were in place. On both ranges the error of measurement was  $\frac{1}{3}\%$  of full-scale deflection. Calibration was by dead weight loading.

A dashpot was connected across the spring system B to prevent resonance vibrations. This gave slightly over critical damping when the springs were stiffened and, consequently, heavy damping when they were not. Even in this case, however, the response time (to 99% of equilibrium deflection) was only 1.5 sec., which was not deleterious.

### 2.3. Performance

The requirement that the glass plate be kept in the field plane of the microscope was well satisfied by the kinematic spring systems. No detectable change of fringe sharpness was observed during the usual sliding experiments in which the glass plate moved 0.1 mm.

The horizontal displacement of the glass plate by the specimen load was about 0.2  $\mu$ /g. when the stiffening blocks were in place and about 0.25  $\mu$ /g.

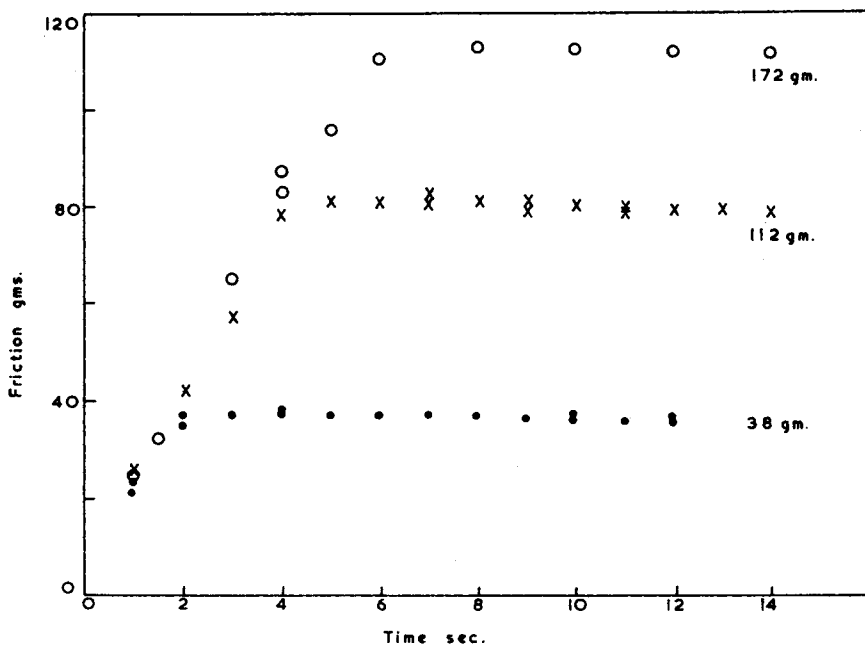


Fig. 2. Variation of friction between nylon 610 specimen and glass plate with time, after application of various loads. At equilibrium the speed of the glass plate was  $9.5 \mu/\text{sec}$ .

when they were removed. Since the depth of field of the microscope was  $\sim 10 \mu$ , refocussing was only essential for large load changes.

A slight inclination between the surface of the glass plate and its direction of motion, amounting to about  $0.5^\circ$ , was largely responsible for the contact area, and the friction, observed for downward motion of the glass plate exceeding their values for upward motion by about 2 and 5%, respectively. To eliminate the effect of this and other, smaller errors, the contact area and friction were measured for both directions of sliding and the arithmetic mean was used.

The vertical deflection of the friction springs was demonstrated to be unaffected by the horizontal load on the glass plate.

The presence of the compliance of the friction-measuring springs between the constant speed drive and the glass plate caused a delay between the application of a load by a specimen onto the glass plate and the achievement of steady sliding. Figure 2 shows the observed dependence of the force indicated by the spring system B on time after application of load. The curves have an initial slope consistent with the glass plate's being at rest relative to the specimen, although the accuracy of the slope is low because of timing errors ( $\pm 1/3$  sec.). The absence of overshoot on the curves suggests that the friction vs. velocity curve for nylon on glass has a positive slope below the equilibrium sliding velocity of  $9.5 \times 10^{-4}$  cm./sec. used in

these experiments. Measurements described in §4.4 confirm this. The standard time of sliding in the main series of measurements was 10 sec. and is seen from Figure 2 to have been quite adequate to ensure that equilibrium sliding was reached in all the present measurements.

#### 2.4. Contact Area Measurement

The apparent contact area between the nylon hemisphere and the glass plate was derived, by the method described in §3.1, from optical interference fringes (Newton's rings) produced around the contact.

A diffuse image of a 250-w. high-pressure mercury arc was thrown onto the contact through the specimen after filtering out heat radiation by 6 mm. of Chance 0N20 glass and isolating the 5461 Å. Hg green line, by means of a Wratten No. 74 filter. The semiangle of the illuminating cone was  $10^\circ$ . Adjustments of the illuminating system were made to give the best compromise between uniformity and intensity of illumination.

Fringes in transmission were employed and were recorded on Kodak microfilm with an exposure of 0.1 sec. Fringe diameters were measured, on projected images of the negatives, to an accuracy corresponding to about  $1 \mu$  at the contact.

The diameter of the apparent contact area was obtained from the diameter of the first-order fringe, by means of a theoretical expression, verified by subsidiary experiments, for the shape of an elastic sphere near the edge of its contact with a rigid plane. The original curvature of the specimen (a parameter entering this expression) was obtained from the fringe pattern observed at loads which produced negligible deformation. The diameter of the apparent contact area ranged from 30 to over 90% of the diameter of the first-order fringe, depending on the load and on the specimen curvature.

### 3. THE CONTACT OF ELASTIC SOLIDS

#### 3.1. Theoretical Predictions about Contacts of Elastic Solids

Hertz<sup>10</sup> derived for the radius of apparent contact  $a$  between two spheres of radius  $R$  under a load  $W$  the following expression:

$$a = [(3/16)WR\theta]^{1/3} \quad (1)$$

where  $\theta = 4(1 - \sigma^2)/E$ ,  $\sigma$  is Poisson's ratio, and  $E$  is Young's modulus.

An explicit expression for the shape into which the spheres distort in the neighborhood of the contact (i.e., the "profile" of the contact) was not given by Hertz but has been calculated by Dr. A. S. Lodge (unpublished) and is that the separation  $2H$  between the surfaces of the spheres as a function of the distance  $r$  from the center of the contact is:

$$2H = (3/8\pi)(W\theta/a)[\epsilon - (1 - \epsilon^2) \tan^{-1} \epsilon] \quad (2)$$

where  $\epsilon = (r^2/a^2 - 1)^{1/2}$  and  $r \geq a$ .

Eliminating  $W$  between eqs. (1) and (2) we obtain:

$$2H = (2a^2/\pi R)[\epsilon - (1 - \epsilon^2) \tan^{-1} \epsilon] \quad (3)$$

So the profile of the contact depends only on the original radius of the sphere and on the radius of the apparent contact. The apparent contact area is by symmetry plane and is perpendicular to the line joining the centers of the two spheres. So, if one of the spheres is replaced by a rigid plane, eq. (1) still gives the apparent contact radius but the separation between the remaining sphere and the plane is then  $H$ .

The radius  $a$  of the apparent contact area between a sphere and a rigid plane can be estimated, if the separation  $H$  at a given radius  $r$  is known, by writing eq. (3) in the form:

$$\pi HR/r^2 = a^2/r^2[\epsilon - (1 - \epsilon^2) \tan^{-1} \epsilon] \equiv Q \quad (4)$$

where  $Q$  is a function of  $a^2/r^2$  only, and all the quantities on the left-hand side are known. So, from a graph of  $Q$  versus  $a^2/r^2$  the value of  $a^2/r^2$  for which  $Q$  equals the observed value of  $\pi HR/r^2$  may be estimated and, hence, the value of  $a$  obtained.

It can be shown that a given error in measuring the interference fringe radius  $r$  least affects the value of  $a$  obtained in this way if  $r/a$  has its smallest value, i.e., if the innermost (the zero-order) fringe is used. But the greater uncertainty of measurements on this fringe, because they involve locating the fringe edge, was considered to outweigh its advantage over the next (i.e., first-order) fringe, so measurements on this fringe were used to estimate the contact radius.

The effect of a tangential force in addition to the normal load has been investigated theoretically by Cattaneo,<sup>11</sup> Mindlin,<sup>12</sup> and Mindlin and Deresiewicz.<sup>7</sup> They show that for the contact of two identical isotropic spheres a tangential force causes no change in the distribution of normal traction over the contact area from that given by an existing normal load and, consequently, the apparent contact area remains plane and unchanged in size.

### 3.2. Experimental Profile

The optical interference fringes (Newton's rings) which are produced round the contact are contours of equal separation between the specimen and the glass plate. The edge of the central bright area (the zero-order fringe) corresponds to a separation of about  $\lambda/8$  and the centers of successive bright annular fringes correspond to  $\lambda/2$ ,  $2\lambda/2$ ,  $3\lambda/2$ , etc. (first-order, second-order, third-order fringes, respectively). Mercury green light of  $\lambda = 5461$  Å. was used. The experimental profile at separations greater than  $\lambda/8$  is therefore readily obtained from the radii of the fringes.

The circles in Figure 3 represent the observed profile of a specimen of radius 0.244 cm. when subjected to a load of 112 g. for 10 sec. The solid line is the theoretical profile for a specimen of this radius whose contact radius has the value derived from the first-order fringe by the method

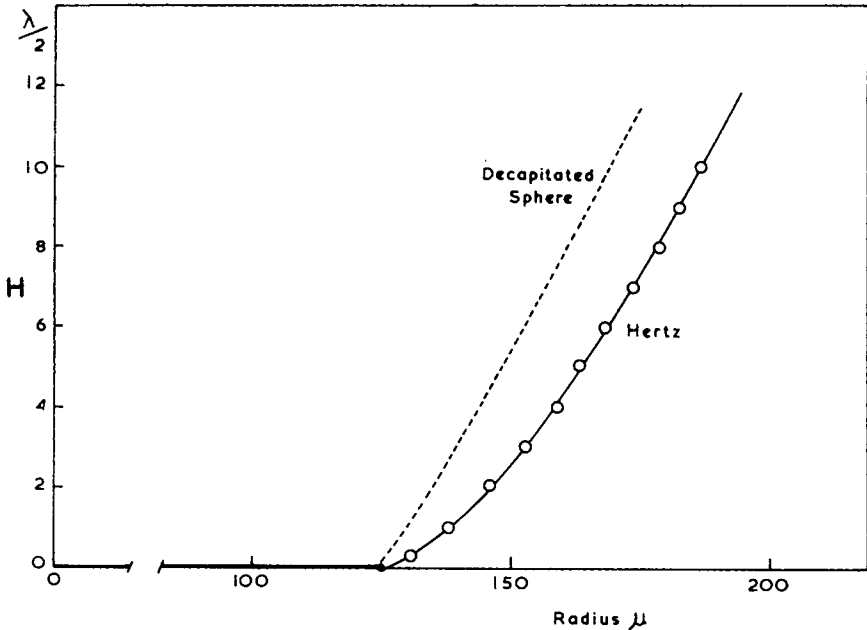


Fig. 3. Profile of a nylon 610 hemisphere pressed against a stationary glass plate: (O) experimental points for a specimen of radius 0.244 cm. under a load of 112 g. for 10 sec. ( $\lambda = 5461$  A.); (—) theoretical profile for an elastically deformed sphere of radius 0.244 cm. fitted to the experimental point for the first-order fringe (i.e.,  $H = \lambda/2$ ); (---) theoretical profile of a sphere of radius 0.244 cm. from which a cap of radius equal to radius of apparent contact area has been removed.

described in §3.1. In effect the theoretical profile has been adjusted to pass through the point representing the first-order fringe. The profile which the specimen would have had if a cap of radius equal to the contact radius had been cut from it is also shown.

The agreement between experiment and theory is very good and similar agreement was found for ratios of  $a/R$  as great as 0.1.

A prominent feature of the theoretical profile is the smallness of the inclination of the specimen surface to the glass plate just outside the edge of the apparent contact area. This can lead, if  $a/R$  is small, to appreciable error if a low-order fringe (even the zero-order) is used as an estimate of the apparent contact area. For example, Lincoln<sup>4</sup> used the zero-order fringe as an estimate of the apparent contact area between a nylon hemisphere of radius 0.158 cm. and a glass plate at loads of 2.6–95 g. Assuming the profile given by eq. (3), we calculate that his estimate is about 80% high at the lowest load and 10% high at the highest load. The correct dependence of apparent contact area is therefore more rapid than he deduced; in fact, calculations based on values taken from Lincoln's Figure 3 suggest that the apparent contact area varies as  $(\text{load})^{0.78}$  rather than  $(\text{load})^{2/3}$  as is suggested there.



### 3.21. Time Effects of Loading and Recovery

Measurements with loading times 5–2400 sec. gave equally good agreement between the theoretical and experimental profiles. Increase in loading time merely leads to the spreading of the fringe pattern, because the apparent modulus of the specimen is reduced.

On removing the load, the specimens recovered virtually completely from deformations in which the ratio  $a/R$  was as great as 0.1, but this recovery took an appreciable time. In one example in which the loading time was 2400 sec., recovery which was complete within experimental error had taken place in 8400 sec. For short loading times the ratio of recovery time to loading time was greater than in this example. During the early part of the recovery the profile differs from both the elastic profile and the original sphere.

### 3.22. Master Profile

The similarity of the profiles of the deformed specimens of different curvatures under different loads can be more easily seen if the profiles are plotted on a master curve. The equation of a suitable master curve can be obtained by rewriting eq. (4) in the form

$$\pi HR/a^2 = [\epsilon - (1 - \epsilon^2) \tan^{-1} \epsilon] \quad (5)$$

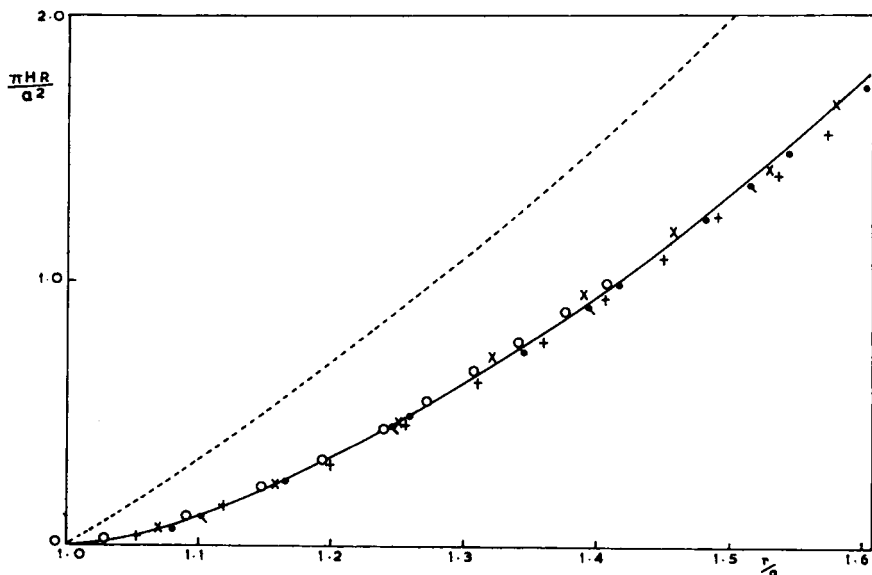


Fig. 4. Master profile of elastically deformed nylon 610 hemispheres: (—)  $\pi HR/a^2 = [\epsilon - (1 - \epsilon^2) \tan^{-1} \epsilon]$  where  $\epsilon = (1 - a^2/r^2)^{1/2}$ ; (---)  $\pi HR/a^2 = (\pi/2)(1 - a^2/r^2)$  approximating to the profile of a decapitated sphere where  $r \ll R$ . In these equations  $R$  = radius of specimen,  $H$  = separation between specimen and glass plate at a distance  $r$  from the center of the contact,  $a$  = radius of the apparent contact area.

Experimental points, loading, radius of specimen in cm.: (×) 38 g., 0.12 cm.; (●) 24 g., 0.24 cm.; (●) 57 g., 0.24 cm.; (O) 172 g., 0.24 cm.; (+) 172 g., 0.52 cm.

Experimentally we know  $H$  as a function of  $r$  (i.e., the fringe order as a function of fringe diameter) and can derive  $R$  and  $a$  from the diameters of the fringes so that we can evaluate  $\pi HR/a^2$  and  $r/a$  from our observations. In Figure 4,  $\pi HR/a^2$  is plotted against  $r/a$  for several specimens. The solid line in this figure is a plot of eq. (5) and is in close agreement with the experimental points.

This good agreement between theory and experiment is surprising, because the theory was derived for Hookean materials but the deformation of the specimens is non-Hookean (see §3.5). This implies that the profile is insensitive to the deformation characteristics of the material and that (most significantly for our present purpose) eq. (3), the theoretical profile, can be used to estimate apparent contact radii for the specimens.

### 3.3. Variation of Contact Area with Loading Time

Pascoe and Tabor<sup>5</sup> have reported that the contact area between a steel ball and a plane polymer surface increases as the logarithm of the loading time. Their estimate of the contact area was the area of the depression

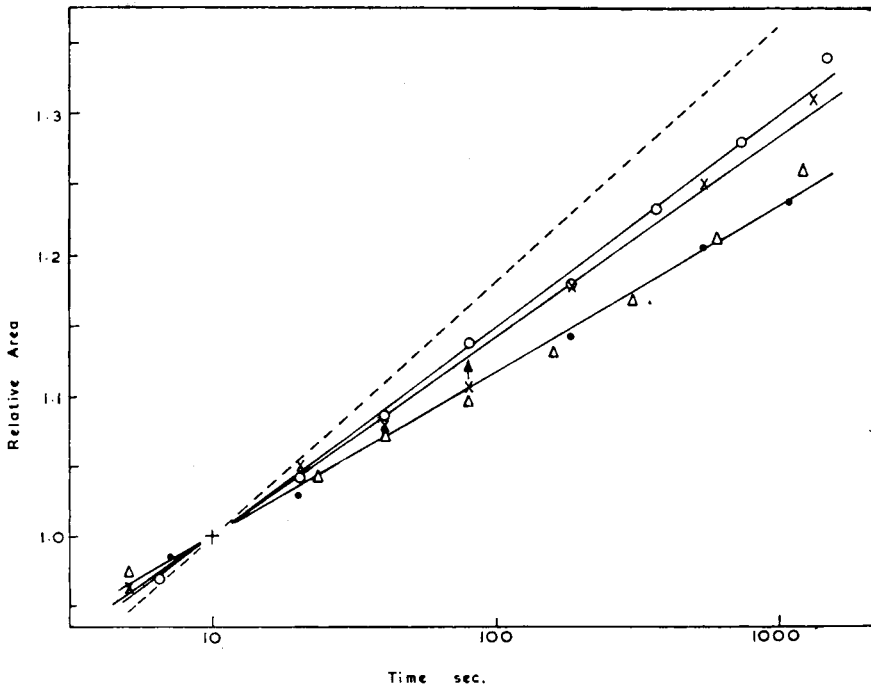


Fig. 5. Growth with loading time of apparent contact area between nylon specimens and a stationary glass plate, expressed as ratio of apparent contact area at time  $T$  to its value when  $T = 10$  sec. The average pressure on the apparent contact area when  $T = 10$  sec. is used as a parameter. Radius of specimen in cm. and pressure ( $P$ ) in  $\text{kg./mm.}^2$ : (●) 0.52 cm.,  $P$  1.8; (Δ) 0.12 cm.,  $P$  1.9; (×) 0.12 cm.,  $P$  2.8; (○) 0.12 cm.,  $P$  4.0; (---) measurements made by Pascoe and Tabor<sup>5</sup> with an indenter of radius 0.5 cm. and a pressure of about  $10 \text{ kg./mm.}^2$  (see § 3.3).

remaining in the polymer after the removal of the load. In the experiments described here the contact area can be measured as a function of time without removing the load. In this case, too, a linear increase of contact area with the logarithm of the loading time was observed. This is illustrated by Figure 5. The dashed line represents the observation of Pascoe and Tabor<sup>5</sup> that the contact area between a 5-mm.-diameter steel ball and a plane nylon surface under a load of 10 kg. increased by 40% as the loading time increased from 6 to 1000 sec. The slopes of the lines show a slight systematic increase with mean pressure.

#### 3.4. Deformation under Combined Normal and Tangential Forces

Normal loads were applied as before for 10 sec. before photographing the interference fringes between the specimen and the glass plate and were removed immediately after the exposure. When tangential forces were required the load was applied while the glass plate was moving at a constant speed (9.5  $\mu$ /sec.). The friction between the specimen and the plate therefore provided the tangential force and its magnitude was recorded on the same film as the interference fringes.

Because the motion of the glass plate was not precisely parallel to its surface but was inclined at an angle of  $\sim 1/2^\circ$  to it, and because of other minor discrepancies of the apparatus, the load on the specimen was slightly different, when sliding took place, from its value when the plate was stationary. This error was small (about 2.5%) and was eliminated by performing measurements with reversal of sliding direction and averaging the results obtained. Photographs were therefore taken under the following sequence of conditions: static, sliding upwards, static, sliding downwards, static, etc. After each measurement the specimen was allowed to relax, without load, for 3 min., which was sufficient for it to recover its original curvature.

From such sets of measurements it is possible to test the predictions that tangential tractions do not affect the shape or magnitude of the contact area.

##### 3.41. *The Effect of Tangential Traction on Contact Shape*

Measurements on fringes whose diameters were only 10–20% greater than that of the apparent contact area showed that the ratio of their diameters parallel to the friction to those in a perpendicular direction increased by only 0.5% with increase of tangential traction from 0 to 2 kg./mm.<sup>2</sup>.

From this we conclude that the greatest tangential traction that occurred in the present measurements had negligible effect on the contact shape.

##### 3.42. *The Effect of Tangential Traction on the Specimen Profile*

It was found that the radii of fringes (of order from 2 to 9) measured in the direction of the friction did not differ by more than 2  $\mu$  (i.e.,  $\sim 1\%$  of

the fringe radius) from those in the opposite direction, even when the apparent contact area was subjected to tangential tractions as great as 2 kg./mm.<sup>2</sup>. The radii were measured from the center of the first-order fringe. A similar analysis for the perpendicular direction showed differences of about half the above value and suggests that both the differences are largely adventitious. Changes of fringe radius of these sizes (which are comparable with errors of measurement), whatever their origin, seem insufficient to affect the use of the theoretical profile of the specimen in the presence of our greatest tangential tractions.

### 3.4.3. The Effect of Tangential Force on Contact Area

In the light of the conclusions of the preceding sections it is permissible to estimate the contact area in the presence of tangential forces by the method that was used in §3.1, when only normal loads acted. Table I gives the contact areas determined in this way from measurements on five different specimens under various normal forces using the routine described in §3.4.

The change of contact area produced by the tangential force shows considerable scatter but it is usually an increase and has an arithmetic mean value of +1.7% in these measurements in which the mean ratio  $F/W$  was 0.51. The magnitude of the area of contact is therefore only very slightly

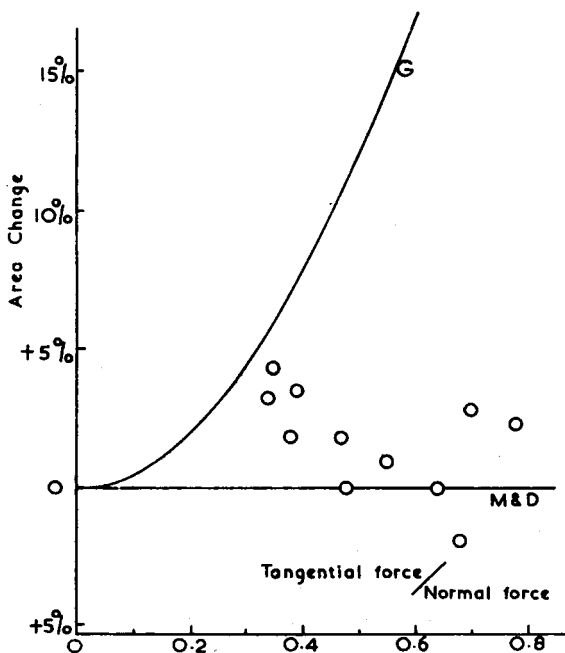


Fig. 6. Effect of tangential force on apparent contact area: (O) experimental values (see Table I). The lines G and M&D represent theoretical predictions of Grosberg<sup>6</sup> and of Mindlin and Deresiewicz,<sup>7</sup> respectively.

affected by the tangential forces produced by friction. A more detailed examination of the results is possible from Figure 6, in which the observed increases of contact area together with the theoretical predictions (of Mindlin and Deresiewicz<sup>7</sup> and of Grosberg<sup>8</sup>) are plotted against the ratio  $F/W$ . The experimental results are clearly inconsistent with the predictions of Grosberg's theory. For high values of  $F/W$  the results are in very good agreement with Mindlin and Deresiewicz's theory, but as  $F/W$  decreases they tend to diverge slightly. Now, the lower values of  $F/W$  were obtained (see Table I) with the greater values of normal load and, consequently, with greater strains of the specimens, so this tendency may indicate the inapplicability at finite strains of the latter theory, which was derived for infinitesimal strains.

TABLE I  
Effect of Friction on Magnitude of Contact Area<sup>a</sup>

$R$ , cm.	$W$ , g.	Area, $10^{-6}$ cm. <sup>2</sup>				$100(A_m - A_s)/A_s$	$S$ , kg./ mm. <sup>2</sup>	$F/W$	$a/R$
		$A_u$	$A_d$	$A_m$	$A_s$				
0.122	8.0	53.9	57.0	55.5	54.2	+2.3	1.12	0.78	0.034
	12.8	68.5	68.5	68.5	68.5	0.0	1.20	0.64	0.038
	172	443	452	447.5	432	+3.5	1.50	0.39	0.096
0.124	12.8	69.1	69.1	69.1	68.5	+0.9	1.01	0.55	0.038
	57	193	194	193.5	190	+1.8	1.12	0.38	0.063
	172	430	442	436	418	+4.3	1.37	0.35	0.093
0.123	8.0	51.1	51.1	51.1	52.1	-2.0	1.06	0.68	0.034
	38.2	142	148	145	145	0.0	1.25	0.48	0.055
	112	283	291	287	282	+1.8	1.85	0.47	0.077
0.124	172	396	404	400	387	+3.2	1.48	0.34	0.090
0.24	172	590	612	601	584	+2.9	2.00	0.70	0.057

<sup>a</sup> Where  $R$  = specimen radius,  $W$  = load,  $A_u$  and  $A_d$  = contact areas measured with sliding upwards and downwards respectively,  $A_m = \frac{1}{2}(A_u + A_d)$ ,  $A_s$  = static contact area,  $S$  = friction per unit contact area ( $F/A_m$ ),  $a$  = radius of contact area.

### 3.5. The Dependence of Contact Area on Load and Specimen Radius

#### 3.51. Load Dependence

Measurements of the dependence of contact area on the load  $W$  have been made over a range of  $W$  of  $\sim 1$  to  $\sim 170$  g. Over this range, for specimens of radii of 0.12–0.66 cm., the contact area varied as  $W^m$  where  $m$  was about 0.7. Figure 7 is a sample double logarithmic plot of contact area versus load for a specimen of radius 0.30 cm., which gave a value of 0.72 for  $m$ . For a Hookean elastic solid, eq. (1) predicts that the contact area will vary as  $W^{2/3}$  and, although the excess of the experimental value of  $m$  over  $2/3$  is small, it persists in measurements with many different specimens.

A mean value of  $m$  was found from the measurements on the fifteen specimens used in the simultaneous measurements of contact area and friction described below in §4. The tangential forces present in these measurements have been shown in §3.43 to have no significant effect on the contact area.

The value of  $m$  was calculated for each specimen as the slope of the best straight line fitted by a least-squares method to the logarithmic values of  $A$  and  $W$ . Errors were assumed to be confined to the area measurements, because the errors in the applied loads were much less than these. In

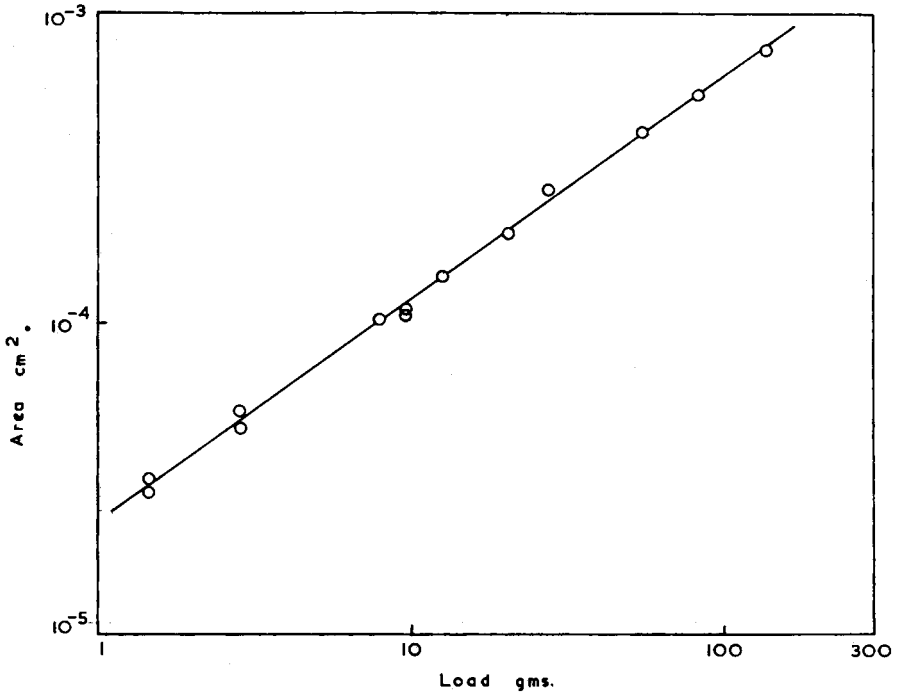


Fig. 7. Apparent contact area, between a nylon specimen of radius 0.30 cm. and a stationary glass plate, as a function of load. Loading time, 10 sec.

effect, the regression of  $\log_{10} A$  on  $\log_{10} W$  was determined. Equal statistical weight was given to each point, since it was found that giving greater weights (arbitrarily selected) to the rather more precisely measured areas obtained with the higher loads had an insignificant effect on the value of  $m$  and little effect on its precision.

The values of  $m$  (see Table II) ranged from 0.664 to 0.732 with a mean of 0.708 and a standard deviation about the mean of  $\pm 0.022$ . Comparison of the root-mean-square, the mean, and the quartile estimates of the spread demonstrated that the distribution of the values was Gaussian. The best estimate of  $m$  is therefore the mean value 0.708 and its standard error is  $\pm 0.006$ .

TABLE II  
Values of  $n$ ,  $m$ , and  $n - m$  for 15 Nylon Specimens

$R$ , cm.	$n$	$m$	$n - m$
0.1245	$0.783 \pm 0.007$	$0.675 \pm 0.006$	0.108
.1233	$.816 \pm 0.011$	$.702 \pm .006$	.114
.1235	$.805 \pm 0.010$	$.689 \pm .005$	.116
.1215	$.726 \pm 0.013$	$.675 \pm .011$	.051
Mean: 0.123	$0.782 \pm 0.020$	$0.685 \pm 0.007$	$0.097 \pm 0.016$
0.241	$0.762 \pm 0.010$	$0.710 \pm 0.007$	0.052
.240	$.806 \pm .017$	$.729 \pm .007$	.077
.244	$.713 \pm .015$	$.664 \pm .007$	.049
.234	$.815 \pm .012$	$.726 \pm .007$	.089
.242	$.799 \pm .012$	$.705 \pm .004$	.094
Mean: 0.240	$0.780 \pm 0.023$	$0.708 \pm 0.012$	$0.072 \pm 0.010$
0.556	$0.822 \pm 0.036$	$0.712 \pm 0.007$	0.110
.638	$.752 \pm .022$	$.707 \pm .014$	.045
.657	$.700 \pm .022$	$.732 \pm .008$	-.032
.544	$.827 \pm .012$	$.729 \pm .005$	.098
.554	$.857 \pm .033$	$.722 \pm .005$	.135
.560	$.724 \pm .018$	$.726 \pm .015$	-.012
Mean: 0.585	$0.780 \pm 0.026$	$0.723 \pm 0.005$	$0.057 \pm 0.028$
Grand mean:	$0.781 \pm 0.012$	$0.708 \pm 0.006$	$0.073 \pm 0.013$

The mean values of  $m$  when grouped according to specimen radius were 0.685, 0.707, and 0.723 for the groups of mean radii 0.123, 0.240, and 0.585 cm., respectively. A similar tendency of the value of  $m$  to increase with radius of curvature may be inferred from Figure 3 of Pascoe and Tabor.<sup>5</sup> Its significance is not known.

### 3.52. Radius Dependence

The dependence of contact area on specimen radius was determined at a normal force near the mean logarithmic value of  $W$ . This choice minimized the influence of errors in the value of  $m$  and also enabled all the measured values of  $A$  and  $W$  to be used, so giving greater accuracy.

For each of the three radius groups of specimens the values of  $\log A$  and  $\log W$  were summed for all the measurements on all the specimens in the group. The values of  $\overline{\log A}$  and  $\overline{\log W}$  obtained in this way are given in columns 2 and 3 of Table III. Because some of the extreme values of normal force were not used on some specimens, so that the three values of  $\overline{\log W}$  were not identical, it was necessary to adjust the values of  $\overline{\log A}$  and use the experimental values of  $\overline{m}$  to a common value of  $\overline{\log W}$ . These adjusted values are given in Column 4. The dependence of  $A$  on  $R$  may now be obtained from a graph of the adjusted values of  $\overline{\log A}$  versus  $\overline{\log R}$  (Fig. 8) whose slope is the power of  $R$  to which  $A$  is proportional. The three points on Figure 8 lie very close to a line of slope 0.576 so that  $A \propto R^{0.576}$ .

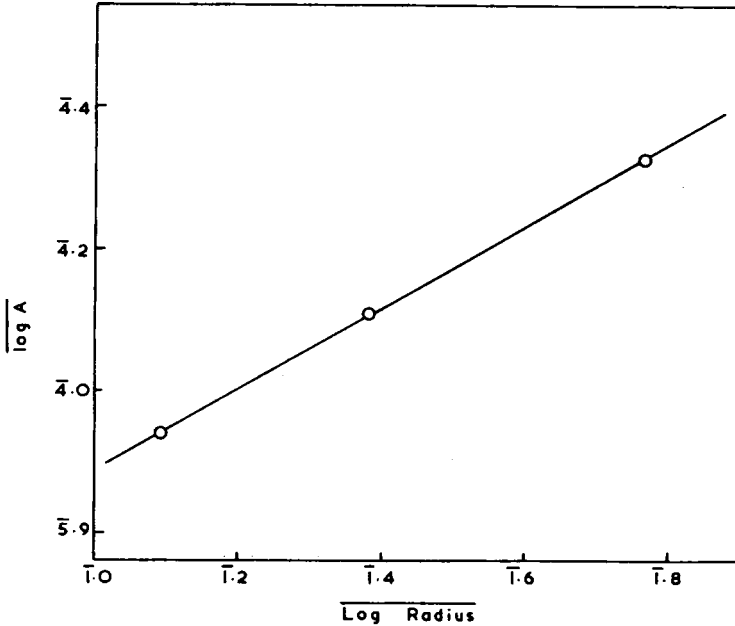


Fig. 8.  $\log_{10}$  apparent contact area versus  $\log_{10}$  specimen radius for nylon specimens pressed against glass plate under equal loads. Loading time 10 sec.

TABLE III  
Dependence of Contact Area on Specimen Radius at Constant Load\*

$\bar{R}$	$\overline{\log A}$	$\overline{\log W}$	$\overline{\log A}$ adjusted	$\log W$ common
0.123	$\bar{5}.958$	1.276	$\bar{5}.940$	1.250
0.240	$\bar{4}.103$	1.238	$\bar{4}.111$	1.250
0.585	$\bar{4}.323$	1.246	$\bar{4}.328$	1.250

\*  $\bar{R}$  = mean radius of specimens in each group,  $\overline{\log A}$  = mean logarithmic area in  $\text{cm.}^2$  for all measurements on specimens in each group,  $\overline{\log W}$  = mean logarithmic load in g. for these measurements.

### 3.53. Comparison of Load and Radius Dependence of Contact Areas

The empirical dependences of apparent contact area on load at constant specimen radius and on radius at constant load, which have been derived in §3.51 and §3.52, may be related by the following dimensional argument. According to the Principle of Geometrical Similarity (Tabor,<sup>13</sup> page 68) the strains and stresses in all specimens (of the same material) which make contacts with the same values of the ratio of contact radius to specimen radius (i.e.,  $a/R$ ) have equal values at corresponding points. Consequently, the average normal pressure on the contact area,  $W/\pi a^2$ , is a



function of the deformation parameter  $a/R$ . Taking this function to be a power law we have

$$W/\pi a^2 = k(a/R)^x \quad (6)$$

where  $k$  is a constant.

On rearranging we obtain

$$\pi a^2 \equiv A = KW^{2/(2+x)} R^{2x/(2+x)} \quad (7)$$

A relation first given by Pascoe and Tabor.<sup>5</sup> Equating the empirical indices of  $W$  and  $R$  from §3.51 and §3.52, i.e., 0.708 and 0.576, respectively, with the indices of  $W$  and  $R$  in eq. (7) we obtain values for  $x$  of 0.82 and 0.81. The similarity of these values obtained in two different ways supports the power law relationship assumed in eq. (6).

It must be borne in mind that, if the tendency of  $m$  to increase with specimen radius (which was mentioned in §3.51) were physically significant, this dimensional argument would be inapplicable.

#### 4. SIMULTANEOUS MEASUREMENT OF FRICTION AND APPARENT CONTACT AREA

The normal measuring routine was to apply the load between the specimen and the glass plate when the glass plate was moving at a constant speed. When this was done the friction-measuring springs deflected at first as if the glass plate had been arrested—i.e., indicated a force increasing linearly with time—until, after a short transition region, the force became constant and steady sliding occurred (see Fig. 2).

If the specimen was pressed against the glass plate before the plate was moved the friction first overshot and then decreased to the steady sliding value when the plate was set in motion. The amount of overshoot increased with the duration of stationary contact.

The effects of variations in the frictional properties of the glass plate from point to point on its surface were reduced by confining all the friction measurements on a specimen to a small region of the glass plate. At the lowest speed the position of the glass plate when the friction was recorded was reproducible to within  $\pm 15 \mu$ , i.e., less than the diameter of the smallest apparent contact area; at the highest speed the reproducibility of position was about 10 times worse.

The optical measurements of §3.21 have shown that the macroscopic deformation of a specimen is elastic, i.e., recoverable. Also, no microscopic damage to the specimen surface was apparent after sliding even though the average tangential traction on the apparent contact area reached 2 kg./mm.<sup>2</sup>. (This conclusion appears to conflict with the observation made by Chapman<sup>14</sup> that, when the average tangential traction between a flat glass slider and a nylon bristle reached values similar to this, heavy tearing of the nylon was produced. Chapman remarks that the damage appeared to start mostly at the leading edge of the slider, and

perhaps the complicated stress distributions near the leading edge were responsible for the tearing.) Furthermore, no transfer of nylon to the glass was observed with the optical microscope, and the friction of a specimen on a part of the glass surface which had been repeatedly rubbed by the specimen was not significantly different from that on an adjoining fresh part of the glass surface.

The measurements of the variation of friction with load were performed at a sliding speed of  $9.5 \mu/\text{sec.}$  with a loading time of 10 sec., so that steady sliding was always achieved. The precise values of these parameters were arbitrary but their orders of magnitude were selected to keep side effects (such as frictional heating—see §4.2) small, to keep timing errors small, and to enable measurements over a full loading cycle to be made for one specimen in one day. (The loading time determines the time the specimen must be allowed to recover before a subsequent measurement. For a loading time of 10 sec. a recovery time of 3 min. was adequate.)

In subsidiary experiments described in §4.3 and §4.4, the effect of varying these parameters was measured. From the results obtained it is concluded that the observed friction-load and contact area—load relations would not have been significantly affected by considerable changes in the chosen sliding speed or loading time.

#### 4.1. Load Dependence of Friction

The load dependence of friction was measured for fifteen specimens whose radii of curvature ranged from 0.12 to 0.66 cm. Simultaneous measurements of friction and apparent contact area were made at each of nine loads from 0.77 to 172 g. At each load the average was taken of the contact area and of the friction measured for upward and downward sliding. This averaging eliminated certain slight residual errors of the apparatus (see §2.3). For loads of 0.77–12 g. the higher friction sensitivity was used, and two sequences of measurements, each with the load increasing through this range, were performed before the friction sensitivity was changed to its lower value. Two similar sequences of measurements at loads overlapping the previous range and extending up to 172 g. were then performed. Repeat measurements of friction, except at the very lowest loads, agreed to within about 3%, although the specimens had been subjected to loads 10 or more times greater between the measurements. The reproducibility of apparent contact area measurements was even better than this.

Some sample double logarithmic plots of friction versus load are shown in Figure 9. It is seen that, except at the lowest loads, the experimental points lie on straight lines, demonstrating that the relation between friction and load is a power law, i.e.,  $F = \alpha W^n$ . The slopes of the lines and hence the indices  $n$  are very similar for these three specimens. At low loads the friction falls below the extrapolation of the power law and the deviation tends to start at higher loads for specimens of larger radius.

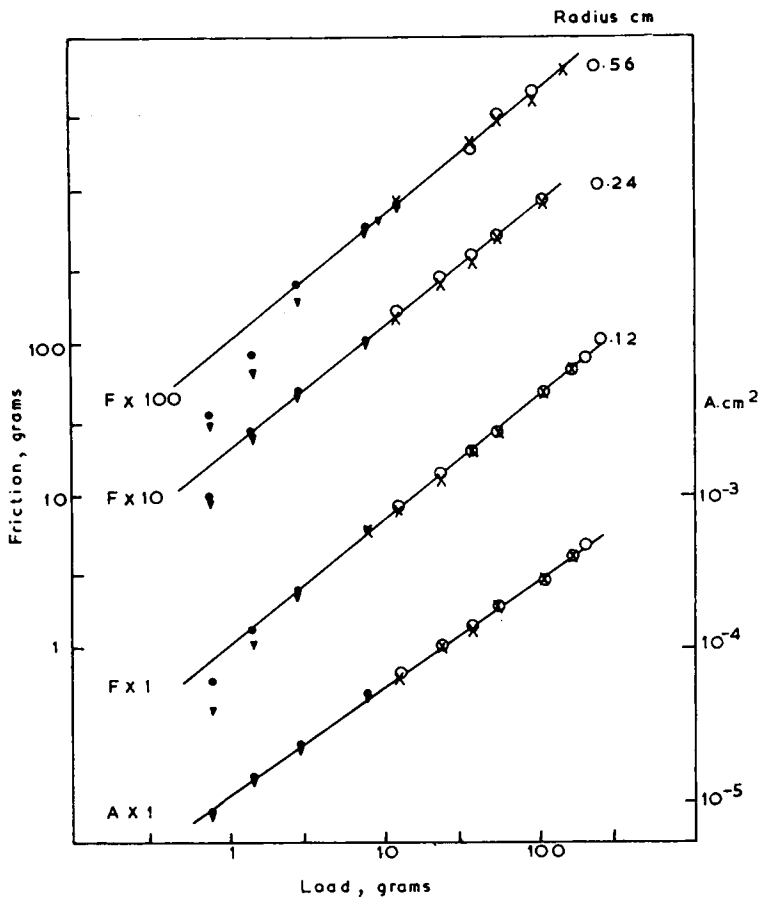


Fig. 9. Dependence of friction and apparent contact area on load for nylon 610 on glass. All measurements at a sliding velocity of  $9.5 \mu/\text{sec.}$  after a loading time of 10 sec. Four series of measurements on each specimen (sequence denoted by symbols  $\nabla$ ,  $\bullet$ ,  $\times$ ,  $\circ$ ) in each of which increasing values of load were used. The lower two lines represent simultaneous measurements of friction and apparent contact area on the same specimen. For clarity, the ordinates of the third and the top lines are increased by one and two decades respectively.

However, over the major part of the load range the power law is obeyed and it is with this part that we are most concerned.

Analysis of the simultaneous apparent contact area measurements (see §3.51) also indicates a power law relationship, i.e., that  $A = \beta W^m$ , but the value of  $m$  is less than the friction index  $n$ . The two lowest lines in Figure 9 are the friction versus load and area versus load plots for the same specimen, clearly illustrating this.

Numerical values of  $n$  for each specimen were obtained by fitting straight lines to the logarithmic values of  $F$  and  $W$  just as was done in §3.51 for  $A$  and  $W$ , to obtain values of  $m$  for these very specimens. Measurements

at loads below 1.4 g. for specimens of radii 0.12 and 0.28 cm. and below 2.8 g. for those of radii about 0.58 cm. were not used. Equal statistical weight was given to each point since the percentage scatter of the experimental points did not change greatly with load. It was confirmed that giving greater statistical weights to the measurements at the higher loads did not significantly affect the slopes of the fitted lines.

Table II contains the values of  $n$  (and of  $m$ ) for the 15 specimens, together with their respective standard deviations calculated from the goodness of fit of the lines. The values of  $n$  range from 0.700 to 0.857 with a mean of 0.781. The standard deviation of the mean is  $\pm 0.012$ . Almost identical mean values of  $n$  are found for each radius group.

We see that the differences  $n - m$  are all positive except for two specimens of the largest radius. The mean value of  $n - m$  is 0.073 with a standard deviation of  $\pm 0.013$  and is statistically highly significant.

#### 4.2. Temperature Rise

An upper limit for the temperature rise at the surface of contact between the specimen and the glass plate after 10 sec. of sliding at the lowest steady sliding speed, i.e.,  $9.5 \mu/\text{sec}$ . (the conditions under which the main series of measurements were performed), was estimated theoretically as  $0.33^\circ\text{C}$ . when the tangential traction had its maximum value of  $2 \text{ kg./mm.}^2$ . In obtaining this estimate it was assumed that the true contact area was approximately equal to the apparent contact area, which is highly likely for such a high value of tangential traction, and that conduction only occurred perpendicular to the contact surface.

A change of temperature of  $0.33^\circ\text{C}$ ., which is comparable to the fluctuations of the ambient temperature, is almost certainly negligible. Experimental confirmation that the temperature rise is negligible at the lowest sliding speed was provided by the absence of a significant friction change, attributable to temperature rise when friction was recorded during continuous sliding from 10 to 60 sec. after application of load. At higher sliding speeds greater temperature rises would be expected but the cooling effect of the fresh glass which the specimen will touch (when the sliding distance exceeds the diameter of the contact) will make the rise less than proportional to speed.

#### 4.3. Loading Time

The effect of loading time on friction was studied by applying the load for known times when the glass plate was stationary and then accelerating and moving the glass plate at constant speed for 10 sec. By this means frictional heating in measurements with widely different loading times was kept small and fairly constant. The sliding time of 10 sec. was adequate for the friction overshoot which was observed under these conditions (see §4) to have decayed and for steady sliding to have been achieved before the friction and contact area were recorded.

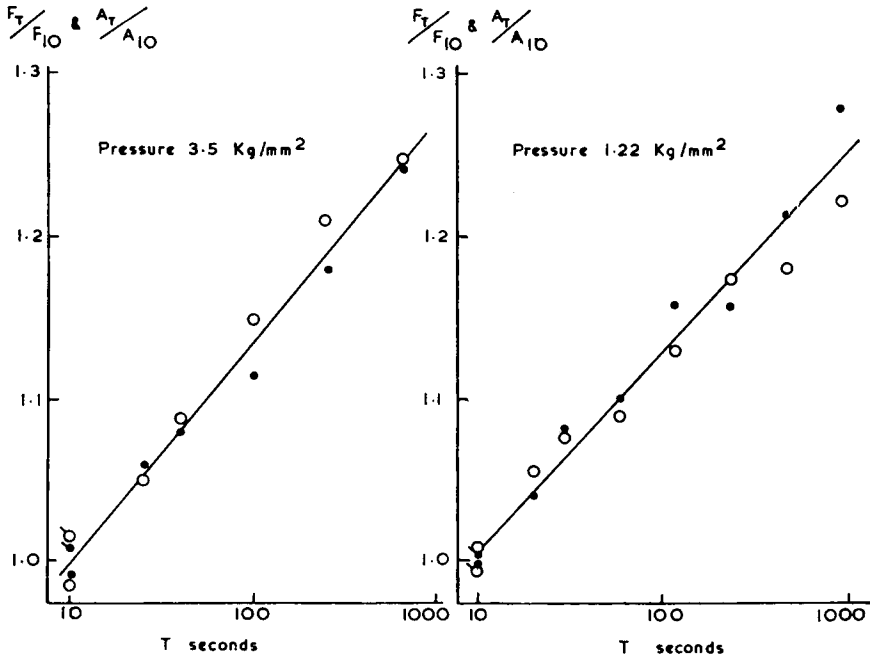


Fig. 10. Growth of apparent contact area and friction with loading time. Ratios of apparent contact area and friction after a time  $T$  to their values when  $T = 10$  sec. for two values of the average pressure on the apparent contact area: (O)  $F_T/F_{10}$ ; (●)  $A_T/A_{10}$ .

Figure 10 shows plots of simultaneous measurements of friction and apparent contact area versus the logarithm of the loading time. Both friction and contact area increase linearly and at nearly the same rate with log time. The increase of contact area is, as would be expected, very similar to that observed in the static loading experiments (§3.31) because the only difference between the experiments is the presence or absence of friction during the last 10 sec.

From Figure 10 the increase of friction for a 100-fold increase of loading time is about 5% greater under a mean pressure of 3.5 kg./mm.<sup>2</sup> than under one of 1.22 kg./mm.<sup>2</sup>. This corresponds to a difference of only 0.012 in the index  $n$  of the equation  $F = \alpha W^n$  between values obtained in the extreme loading times of this experiment. The index  $m$  of the apparent contact area equation  $A = \beta W^m$  is even less affected.

We may conclude that substantially the same dependences of contact area and friction on load would have been observed throughout this 100-fold range of loading time, so that the particular value chosen for the standard loading time is immaterial.

#### 4.4. Sliding Speed

Two methods were used to study the variation of friction with sliding speed. One, which employed steady sliding, was used for speeds of

9.5–330  $\mu$ /sec. The other, which employed the transient motion observed when steady sliding was terminated, permitted the speed range to be extended downwards to about  $10^{-7}$  cm./sec.

#### 4.41. High Speeds

Continuous sliding at six speeds in the range 9.5–330  $\mu$ /sec. was produced by a gear box in the drive between the motor and the lead screw.

Measurements taken at speeds decreasing from the maximum usually showed that the friction was 5 or 10% greater than when an increasing sequence of speeds was used. This behavior was not, however, universal and this hysteresis tended to be small in a second cycle and was also usually small for specimens which had been repeatedly rubbed at low speeds. The differences were possibly caused by frictional heating at the highest speeds; the reproducibility of the friction at low speeds (§4.42) was much better.

#### 4.42. Low Speeds

Estimates of the friction at sliding speeds below 9.5  $\mu$ /sec. were made from the transient motion of the glass plate when the motor was switched

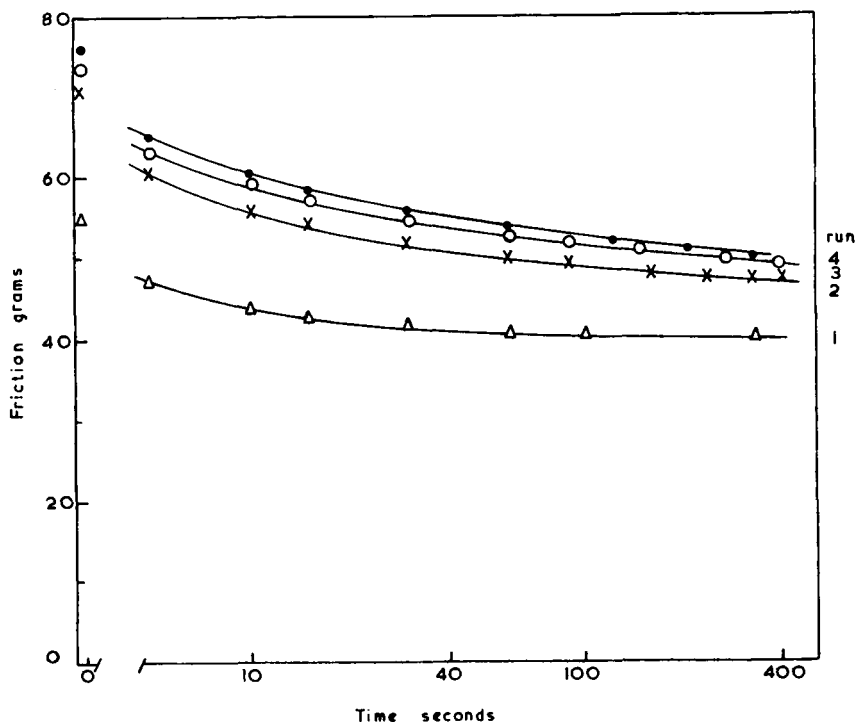


Fig. 11. Decrease of friction with time after stopping of motor which had been generating a sliding speed of 9.5  $\mu$ /sec. Plots of successive runs (in numerical order) in which a nylon 610 hemisphere of radius 0.24 cm. was pressed against a glass plate under a load of 172 g.

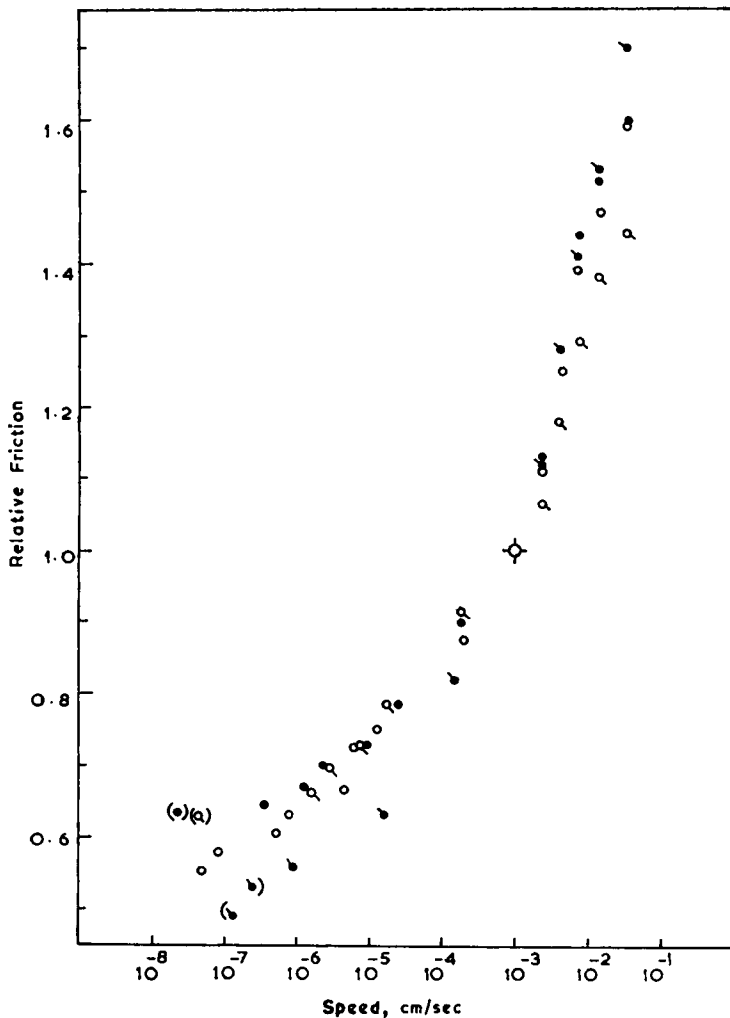


Fig. 12. Speed variation of friction, expressed as its ratio to the friction at a speed of  $9.5 \mu/\text{sec}$ . Specimen radius in cm., load in g., pressure ( $P$ ) in  $\text{kg./mm.}^2$ : ( $\odot$ ) 0.24 cm., 2.8 g.,  $P$  0.8; ( $\bullet$ ) 0.24 cm., 172 g.,  $P$  2.70 ( $\circ$ ) 0.55 cm., 2.8 g.,  $P$  0.5; ( $\circ$ ) 0.55 cm., 38 g.,  $P$  1.1.

off. On stopping the motor without releasing the load the deflection of the friction-measuring spring (which had been essentially constant during the previous steady sliding) decreased with time, at first rapidly and then more slowly, until after a few minutes significant changes could not be observed. Both the friction and the sliding speed during the transient motion can be calculated from records of the variation of deflection with time. Figure 11 shows some typical decay curves. Because even the initial time constant of the decay of deflection is long compared with the natural period of vibration ( $\sim 0.1$  sec.) of the glass plate mounted on the friction-measuring

springs, inertial forces can be neglected, so that the observed deflection is a reliable estimate of the friction. Also, because the top of the friction-measuring springs is at rest relative to the specimen, when the motor has stopped, the relative velocity of the glass plate and the specimen equals the rate of contraction of the spring. (The compliance of the specimen is small compared with that of the spring and has been neglected here.)

Records of the spring deflection were made photographically at increasing time intervals and from each consecutive pair of photographs the mean friction and the mean speed in the intervening time were calculated.

During the friction decay, the specimen remains subject to the normal load and the apparent contact area increases continuously. A correction was therefore needed to refer the friction to the contact area after the standard 10-sec. loading, and was derived either from simultaneous area measurements or from the well-established dependence of contact area on loading time (see §3.31 and §4.2). The correction (to be subtracted) was about 20% at the end of the observed friction decay which lasted about 10 min. If a friction decay experiment was performed on a specimen which had been loaded for a time that was long compared with the duration of the decay, so that the growth of area during it was small, the friction at any time was, of course, greater than if the minimum loading time had been used, but the proportional decrease with time was the same as for the experiments with the corrections above. When the growth of contact area was slow the friction decay curves were remarkably consistent: cf. the top curves of Figure 11, which were consecutive decays (without removal of load) on the same specimen.

Figure 12 is a plot of friction versus  $\log_{10}$  speed, combining the speed ranges covered by the above techniques for two specimens, each under two different loads. For ease of comparison the four measurements have been adjusted to equality at the arbitrary standard speed of 9.5  $\mu$ /sec. It is clear that considerable changes in the sliding speed would not affect the observed dependence of friction on load which was studied at that speed.

## DISCUSSION

### 5.1. Deformation of Nylon

In an investigation of contact deformation of polymers, Pascoe and Tabor<sup>5</sup> measured the areas of indentations produced by steel balls in plane polymer surfaces, a system analogous to the one used in the present work. They showed that the expression  $A = KW^{2/(2+x)}R^{2x/(2+x)}$  (see §3.53) fitted their observations and determined the best value of the parameter  $x$ . They obtained a value of  $x = 0.7$  (corresponding to  $m = 0.74$ ) for nylon 66, and other values in the range 0.4–0.7 for six other polymers. The measurements described in this paper (§3.5) which gave  $x = 0.82$  (i.e.,  $m = 0.708$ ) were on a different nylon (nylon 610), and used deformations about an order of magnitude smaller than those of Pascoe and Tabor, so closer agreement would not be expected.



The effects of loading time observed by Pascoe and Tabor were similar to those described in this paper (see §3.3).

Lincoln,<sup>4</sup> using a technique similar to that of this paper but accepting the zero-order fringe as an estimate of the apparent contact area, showed that  $m = 2/3$  for nylon 66. The criticism (in §3.2) of this method of contact area estimation suggests that this value of  $m$  should be increased to about 0.78. In a later paper, Lincoln<sup>15</sup> reported measurements at higher loads (up to 60 kg. on a 0.158-cm. specimen) which indicated a progressive increase of  $m$  with load. Part of this increase of  $m$  was probably the consequence of reduced systematic error in area measurement at higher loads.

Laws<sup>16</sup> measured the contact area between a nylon filament, encircling a glass rod, and a plane glass surface over a very large ( $10^4$  to 1) range of load. (From the published interferograms the filament appears to have been highly drawn nylon 66.) A plot of log contact area versus log load produced a curve whose tangent (i.e.,  $m$ ) at low loads was  $\sim 0.78$  and at high loads was  $\sim 1.0$ . The interpretation of this increase of slope as indicating a transition from an elastic to a plastic deformation law appears to be inconsistent with the measurements of Pascoe and Tabor,<sup>5</sup> which show no sign of such a transition although they used contact pressures twice as great as any used by Laws. Possibly, in this case too, the use of the zero-order fringe was responsible for some of the apparent increase of  $m$  with load. The method of mounting the filament may also have had a similar effect because, with increase of load, the filament would be progressively squashed between the glass rod and the glass plate, so that the curvature of its axis would tend to decrease.

On the whole, these investigations agree in showing that the index  $m$  for nylon is greater than  $2/3$  which is the theoretical value for a Hookean material. The work of Pascoe and Tabor<sup>5</sup> and of the present author also shows that a consistent representation of the deformation of nylon (including the effect of specimen radius) can be given by a power-law relation between stress and deformation.

## 5.2. Friction of Nylon

The friction measurements made by Pascoe and Tabor<sup>5</sup> showed that for nylon 66 (and other polymers) the dependence of friction on load and specimen radius was approximately the same as the dependence of apparent contact area on these variables. The friction and the contact area measurements were performed separately. Their work was intended as a broad study of polymer friction, and in the case of nylon the specimens used included commercially produced filaments of a wide range of radii whose surface textures probably differed considerably. Small differences between friction and contact area dependences would not therefore be readily detected.

In the present work, both the friction and the contact area measurements were performed with the same specimens so that differences between  $n$  and  $m$  could be more easily detected, and it was found that  $n$  was significantly

greater than  $m$ . Despite the care that was taken to prepare the specimens under identical conditions, the friction of apparently identical specimens under the same load differed considerably. This interspecimen variation probably is attributable to contaminant films (adsorbed on the specimen and the glass plate from the humid laboratory atmosphere in which the experiments were performed) which were not identical for all specimens. This variation made it impracticable to determine the effect of specimen radius on friction with the restricted range of specimen radius which was used.

Lincoln<sup>4</sup> observed that, for a nylon 66 hemisphere of radius 0.158 cm. sliding on glass,  $n$  was  $2/3$ . Now, the value he reported for  $m$  was also  $2/3$ , but if the correction suggested in §3.2 is adopted  $m$  would be increased to 0.78 and we would be faced with the surprising situation of  $m$  exceeding  $n$ .

### 5.3. Speed Dependence of Friction

The measurements described in §4.4 show that the friction of nylon on glass increases continuously with speed throughout the range  $10^{-7}$  to  $3.3 \times 10^{-2}$  cm./sec. (No reliable indication of the behavior at speeds below  $10^{-7}$  cm./sec. is possible with the present apparatus, chiefly because temperature fluctuations of the apparatus would cause irregular variations of the sliding velocity of this order of magnitude.) A maximum in the friction-speed curve, which seems to be required to explain the friction overshoot observed when the specimen and glass plate were pressed together before relative motion was initiated, could therefore only occur at speeds of less than  $10^{-7}$  cm./sec.

Measurements comparable to those described here were performed by Schallamach<sup>17</sup> with rubber on ground glass and on silicon carbide cloth in the speed range  $10^{-4}$  cm./sec. and upwards, and show (particularly those on silicon carbide cloth) a very similar speed dependence. Schallamach also observed a positive temperature coefficient for the friction of rubber, and was led to suggest that frictional sliding is a rate process based on an activation mechanism somewhat similar to Eyring's theory<sup>18</sup> of non-Newtonian flow. Bartenev<sup>19</sup> discusses a similar model to explain the friction-speed dependence of polymer friction. Very similar dependences of friction on speed are obtained for both models; in particular, both predict an essentially linear dependence for large forces. This is shown by Schallamach's measurements for rubber on ground glass but not by those for rubber on silicon carbide cloth nor for the present measurements for nylon on glass, which both cover much greater velocity ranges and show a marked nonlinear dependence (see Fig. 12). Some further elaboration of this molecular theory seems necessary to explain these observations.

## 6. CONCLUSIONS

The major conclusion of this work is that the indices  $m$  and  $n$  in the equations  $A = \beta W^m$  and  $F = \alpha W^n$ , which represent the dependences of

apparent contact area and friction on load, are unequal,  $n$  exceeding  $m$  by 0.073. This implies that the ratio  $F/A$  is not constant but increases slowly with load, as  $W^{0.073}$  or, more significantly, with mean pressure  $\bar{P}$  on the apparent contact area, as  $\bar{P}^{0.25}$ . The mean pressures employed range from 0.5 to 4 kg./mm.<sup>2</sup>.

This increase of  $F/A$  with pressure could be explained either by an increase in the ratio of true to apparent contact area with pressure while there is retained a constant shear strength of the true contact area, or by an increase of this shear strength with pressure.

Although, a priori, the first alternative appears more likely because physical surfaces can never be ideally smooth, a detailed discussion of elastic asperity theories of friction, which is given in the following paper, concludes that the second explanation must be adopted.

The friction of nylon on glass, at constant load, increases with speed throughout the range studied,  $10^{-7}$  to  $3 \times 10^{-2}$  cm./sec., the overall increase being by a factor of about 3. The same speed dependence was found for widely varying loads involving a 5-1 range of mean contact pressures.

The effect of friction forces on the apparent contact area between a nylon hemisphere and a rigid plane surface is shown to be zero within experimental error if the deformation ratio  $a/R$  of the specimen is small ( $\leq 0.06$ ), but for larger deformations ( $a/R \sim 0.1$ ) there is a slight tendency of the apparent contact area to be increased by friction. The null effect observed for small values of  $a/R$  agrees with the predictions of small strain theories for Hookean specimens.

This work forms part of a program of fundamental research undertaken by the British Rayon Research Association.

### References

1. Howell, H. G., and J. Mazur, *J. Textile Inst.*, **44**, T59 (1953).
2. Bowden, F. P., and D. Tabor, *Friction and Lubrication of Solids*, Clarendon, Oxford, 1954.
3. Lodge, A. S., and H. G. Howell, *Proc. Phys. Soc. London*, **67B**, 89 (1954).
4. Lincoln, B., *Brit. J. Appl. Phys.*, **3**, 260 (1952).
5. Pascoe, M. W., and D. Tabor, *Proc. Roy. Soc. London*, **A235**, 210 (1956).
6. Parker, A. C., and D. Hatch, *Proc. Phys. Soc. London*, **63B**, 185 (1950).
7. Mindlin, R. D., and H. Deresiewicz, *J. Appl. Mech.*, **75**, 327 (1953).
8. Grosberg, P., *J. Textile Inst.*, **46**, T233 (1955).
9. Jones, R. V., *J. Sci. Inst.*, **28**, 38 (1951).
10. Hertz, H., *J. reine angew. Math.*, **92**, 156 (1881).
11. Cattaneo, C., *Atti Accad. Naz. Lincei, Rend.*, Ser. 6, **27**, 342, 434, 474 (1938); cited by R. D. Mindlin and H. Deresiewicz, *J. Appl. Mech.*, **75**, 327 (1953).
12. Mindlin, R. D., *J. Appl. Mech.*, **71**, 259 (1949).
13. Tabor, D., *Hardness of Metals*, Clarendon, Oxford, 1951, p. 67.
14. Chapman, J. A., Ph.D. Thesis, Cambridge, 1954.
15. Lincoln, B., *Wool Research*, 2, Wool Industries Research Association, Leeds, 1955, p. 173.
16. Laws, V., *J. Textile Inst.*, **49**, T357 (1958).

17. Schallamach, A., *Proc. Phys. Soc. London*, **65B**, 657 (1952); *ibid.*, **66B**, 386 (1953); *Wear*, **1**, 384 (1958).
18. Eyring, H., *J. Chem. Phys.*, **4**, 283 (1936).
19. Bartenev, G. M., *C. R. Acad. Sci. USSR*, **96**, 1161 (1954).

### Synopsis

An apparatus which permits the simultaneous measurement of kinetic friction and contact area between polymer hemispheres and a smooth glass surface has been used to study the dependence of friction and contact area on load, specimen radius, sliding speed, and loading time. Hemispherical nylon 610 specimens of radii 0.12–0.58 cm. have been used with loads of 0.7–200 g. and sliding speeds from  $10^{-7}$  to  $3 \times 10^{-2}$  cm./sec. All measurements were performed in air at 20°C. and 66% r.h. The contact area was estimated from optical interference fringes (Newton's rings) between the surface of the specimen and that of the glass plate, by means of a theoretical expression, experimentally verified, for the shape into which an elastic hemisphere is deformed when pressed against a rigid plane. The contact area was negligibly affected in size or shape by the presence of the tangential force of friction, in accord with the theory for the contact of elastic spheres. The deformations of the specimens were, within experimental error, completely recoverable but depended on the time of loading. The effects of changes in the four variables, load, radius, speed, and time were found to be essentially independent. Subsidiary experiments showed that both friction and contact area increased by about 10% for each factor-of-10 increase in loading time in the range 5–1000 sec. and that friction increased by a factor of 3 as sliding speed increased from  $10^{-7}$  to  $3 \times 10^{-2}$  cm./sec. The main series of measurements (at constant sliding speed and loading time) showed that the dependence on load  $W$  of both the contact area  $A$  and the friction  $F$  could well be represented by the expressions:  $A = \beta W^m$  and  $F = \alpha W^n$  (where  $\alpha$  and  $\beta$  were constants for a given specimen). The values of  $m$  and  $n$  were almost independent of specimen radius and their mean values, for 15 specimens, were  $0.708 \pm 0.006$  and  $0.781 \pm 0.012$ , respectively. The difference between these values,  $0.073 \pm 0.013$ , is statistically highly significant and in the following paper is interpreted as implying that the friction per unit area of true contact between nylon and glass increases with pressure. The dependence of  $A$  on the specimen radius  $R$  (which is included in  $\beta$ ) was found to be as  $R^{0.876}$ . The value of this index of  $R$  and the value of  $m$  are both consistent with a power-law dependence of mean contact pressure on deformation (measured by the ratio of contact to specimen radius) with index 0.82. The values of  $\alpha$  for specimens of the same radius showed too much variation for a useful estimate of the dependence of  $F$  on  $R$  to be obtained.

### Résumé

Un appareil qui permet la mesure simultanée du frottement cinétique et de la surface de contact entre des hémisphères de polymère et une surface de verre poli, fut employé à l'étude de la dépendance friction et surface de contact, sur les charge, rayon de l'échantillon, vitesse de glissement et temps de charge. On fit usage d'échantillons hémisphériques de nylon 6.10 à rayon de 0.12 à 0.58 cm en charges de 0.1 à 200 gr et des vitesses de glissement de  $10^{-7}$  à  $3 \times 10^{-2}$  cm/sec. Toutes les mesures furent faites à 20°C et 66% d'H.R. La surface de contact fut calculée à partir du contour de l'interférence optique (anneaux de Newton) entre la surface de l'échantillon et celle de la plaque en verre, par une relation théorique, qui fut vérifiée expérimentalement pour la forme dans laquelle une hémisphère élastique est déformée quand on le comprime contre un plan rigide. La surface de contact est peu affectée en dimension ou forme par l'effet d'une force tangentielle de friction, en accord avec la théorie pour le contact de sphères élastiques. Les déformations des spécimens sont entièrement reproductibles, sauf erreurs expérimentales, mais dépendent du temps de charge. On trouvera que les effets de changement des quatre variables c.à.d. charge, rayon, vitesse et temps sont essentiellement indépendants. Des expériences supplémentaires ont montré que le frottement autant que la surface de contact augmentent d'environ 10% pour chaque

augmentation d'un facteur 10 en temps de charge, dans le domaine de 5–1000 sec., et que le frottement augmente d'un facteur 3 quand la vitesse de glissement augmente de  $10^{-7}$  à  $3 \times 10^{-2}$  cm/sec. La série principale de mesures (à vitesse de glissement et temps de charge constants) montre que la dépendance de la charge,  $W$ , tant de la surface de contact ( $A$ ) que du frottement,  $F$ , peut être représentée par les équations:  $A = \beta W^m$  et  $F = \alpha W^n$ , où  $\alpha$  et  $\beta$  sont constants pour un échantillon donné. Les valeurs de  $m$  et  $n$  sont généralement indépendantes du rayon de l'échantillon et ses valeurs principales pour 15 spécimens, étaient respectivement de  $0.708 \pm 0.006$  et  $0.781 \pm 0.012$ . La différence entre ces valeurs, c.à.d.  $0.073 \pm 0.013$  est hautement significative au point de vue de la statistique et dans une prochaine communication on démontrera que le frottement par unité de surface de contact réel entre le nylon et le verre augmente en fonction de la pression. On trouve que la dépendance de  $A$ , du rayon de l'échantillon,  $R$ , (qui est compris dans  $\beta$ ) est  $R^{0.576}$ . Les valeurs de cet exposant de  $R$  et la valeur de  $m$  s'accordent toutes deux, selon une expression régissant des forces de pressions moyennes de contact sur la déformation (mesurée par la relation contact-rayon de l'échantillon) avec une puissance 0.82. Les valeurs de  $\alpha$  pour les échantillons d'un même rayon présentent une trop grande variation pour qu'une estimation utile de la dépendance de  $F$ , en fonction de  $F$ , puisse être obtenue.

### Zusammenfassung

Ein Apparat, der die gleichzeitige Messung der kinetischen Reibung und der Kontaktfläche zwischen Polymerhalbkugeln und einer glatten Glasoberfläche erlaubt, wurde zur Untersuchung der Abhängigkeit von Reibung und Kontaktfläche von Belastung, Probenradius, Gleitgeschwindigkeit und Belastungsdauer verwendet. Untersucht wurden halbkugelige Nylon-6-10-Proben mit Radien von 0,12 bis 0,58 cm, bei einer Belastung von 0,7 bis 200 g und einer Gleitgeschwindigkeit von  $10^{-7}$  bis  $3.10^{-2}$  cm/sek. Alle Messungen wurden unter Luft bei 20°C und 66% rel. Feuchtigkeit ausgeführt. Die Kontaktfläche wurde aus optischen Interferenzstreifen (Newtonschen Ringen) zwischen der Proben- und Glasoberfläche bestimmt und zwar mittels eines theoretischen, experimentell bestätigten Ausdrucks für die Gestalt, die eine elastische Halbkugel beim Pressen gegen eine starre Ebene annimmt. In Übereinstimmung mit der Theorie für den Kontakt elastischer Kugeln konnte die Beeinflussung von Grösse oder Gestalt der Kontaktfläche durch die tangentielle Reibungskraft vernachlässigt werden. Die Verformung der Proben wurde zwar innerhalb der Versuchsfehler vollkommen zurückgebildet, hing aber von der Belastungsdauer ab. Die Einflüsse der Änderung der vier Variablen, nämlich Belastung, Radius, Geschwindigkeit und Dauer erwiesen sich im wesentlichen als von einander unabhängig. Versuche zeigten, dass Reibung und Kontaktfläche für jede Verzehnfachung der Belastungsdauer im Bereich von 5 bis 1000 sek um etwa 10% zunahm und dass die Reibung bei Anwachsen der Gleitgeschwindigkeit von  $10^{-7}$  auf  $3.10^{-2}$  cm/sek um etwa einen Faktor 3 zunahm. Die Hauptmessreihe (bei konstanter Gleitgeschwindigkeit und Belastungsdauer) zeigte, dass die Abhängigkeit der Kontaktfläche,  $A$ , und der Reibung,  $F$ , von der Belastung,  $W$ , durch die Ausdrücke:  $A = \beta W^m$  und  $F = \alpha W^n$  (wo  $\alpha$  und  $\beta$  für eine gegebene Probe Konstante sind), gut dargestellt werden kann. Die  $m$ - und  $n$ -Werte waren von Probenradius praktisch unabhängig und die Mittelwerte für 15 Proben lagen bei  $0,708 \pm 0,006$  bzw.  $0,781 \pm 0,012$ . Der Unterschied zwischen diesen Werten, nämlich  $0,073 \pm 0,013$  ist statistisch durchaus von Bedeutung und wird in der folgenden Arbeit dahingehend interpretiert, dass die Reibung pro Flächeneinheit wahrer Kontaktfläche zwischen Nylon und Glas mit dem Druck zunimmt. Die Abhängigkeit von  $A$  vom Probenradius,  $R$ , (die in  $\beta$  enthalten ist) ergibt sich zu  $R^{0,576}$ . Der Wert dieses Exponenten und der Wert von  $m$  stimmen beide mit einer Potenzgesetzabhängigkeit des mittleren Kontaktdruckes von der Verformung (gemessen durch das Verhältnis von Kontakt- zu Probenradius) mit dem Exponenten 0,82 überein. Die Werte von  $\alpha$  zeigten bei Proben mit dem gleichen Radius zu starke Schwankungen, um für eine Bestimmung der Abhängigkeit von  $F$  von  $R$  brauchbar zu sein.

Received September 10, 1962